THE JOURNAL OF PHYSICAL CHEMISTRY B
A JOURNAL OF THE AMERICAN CHEMICAL SOCIETY

pubs.acs.org/JPCB
Article

The Solvent-Dependent Photophysics of Diphenyloctatetraene

Published as part of The Journal of Physical Chemistry virtual special issue "Early-Career and Emerging Researchers in Physical Chemistry Volume 2".

Daniel W. Polak, Alexandros D. P. Hannon, Guilherme A. Marczak Giorio, Olivia A. Hawkins, and Thomas A. A. Oliver*

Cite This: J. Phys. Chem. B 2023, 127, 8199–8207
Read Online

ACCESS | Metrics & More | Article Recommendations | Supporting Information

ABSTRACT: Despite many decades of study, the excited state photophysics of polyenes remains controversial. In diphenylpolyenes with conjugated backbones that contain between 2 and 4 double carbon−carbon bonds, the first two excited electronic states are nearly degenerate but of entirely different character, and their energy splitting is strongly dependent on solvent polarizability. To examine the interplay between these different states, steady-state and time-resolved fluorescence spectroscopies were used to undertake a comprehensive investigation of diphenylocatetraene's (DPO) excited state dynamics in 10 solvents of different polarizabilities and polarities, ranging from weakly interacting alkanes to polar hydrogen-bonding alcohols. These data revealed that photopreparation of the optically bright $1B_u$ state resulted in fast (<170 ps) internal conversion to the lower-lying optically dark $2A_g$ state. The $2A_g$ state is responsible for almost all the observed DPO fluorescence and gains oscillator strength via vibronic intensity stealing with the near-degenerate $1B_u$ state. The fluorescence lifetime associated with the $2A_g$ state decayed monoexponentially (4.2−7.2 ns) in contrast to prior biexponential decay kinetics reported for similar polyenes, diphenylbutadiene and diphenylhexatriene. An analysis combining the measured fluorescence lifetimes and fluorescence quantum yields (the latter varying between 7 and 21%) allowed for a 190 cm^{-1} Herzberg−Teller vibronic coupling constant between the $1B_u$ and $2A_g$ states to be determined. The analysis also revealed that the ordering of electronic states remains constant in all the solvents studied, with the $2A_g$ state minimum always lower in energy than that of the $1B_u$ state, thus making it a relatively simple polyene compared to structurally similar diphenylhexatriene.

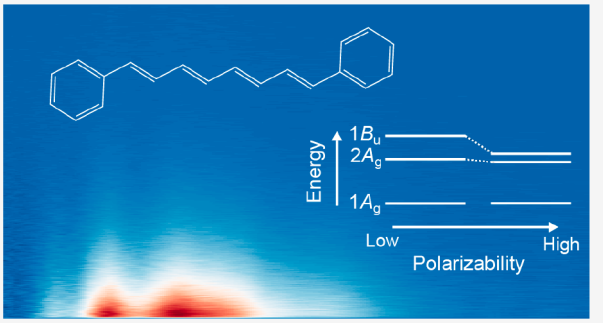

1. INTRODUCTION

Polyenes are an important class of π-conjugated molecules which play a crucial dual role in photosynthesis, acting as accessory light-harvesting pigments and photoprotective radical quenchers.[1−6] Despite several decades of spectroscopic study, the photophysics of polyenes continue to be popular, in part, because their complex electronic structure is still highly debated and varies strongly with chain length, chemical substitution, and environment.[1−3,7−11] The low-energy photophysics of many polyenes is governed by the interconversion between two excited electronic states with different symmetries in the C_{2h} point group.[2,12−14] The electronic ground state of polyenes has A_g symmetry (corresponding to the $1A_g$ state), and the lowest energy optically "bright" electronic state has B_u symmetry ($1B_u$ state).[2,15,16] Early seminal work by Hudson and Kohler[13] proposed that a low-lying electronic state of A_g symmetry (henceforth referred to as the $2A_g$ state) is also important but is formally electrically dipole forbidden and thus termed optically "dark" (see Figure 1a).[11,17−23]

The excitation energies associated with the $2A_g$ and $1B_u$ states are stabilized as the number of double bonds (N) in the polyene backbone increases.[3,23−25] However, due to the differences in electronic character, the stabilization energy per double bond is greater for the $2A_g$ state. As a result, for shorter polyenes with conjugation lengths of $\sim N \leq 2$, such as

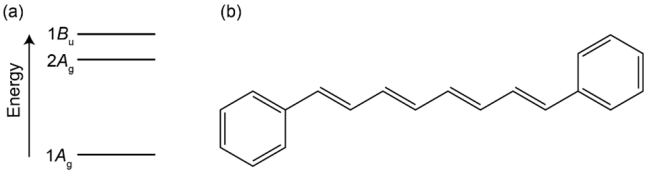

Figure 1. (a) Schematic energy level structure and (b) chemical structure of diphenyloctatetraene (DPO).

Received: June 2, 2023
Revised: August 20, 2023
Published: September 14, 2023

https://doi.org/10.1021/acs.jpcb.3c03737
J. Phys. Chem. B 2023, 127, 8199−8207

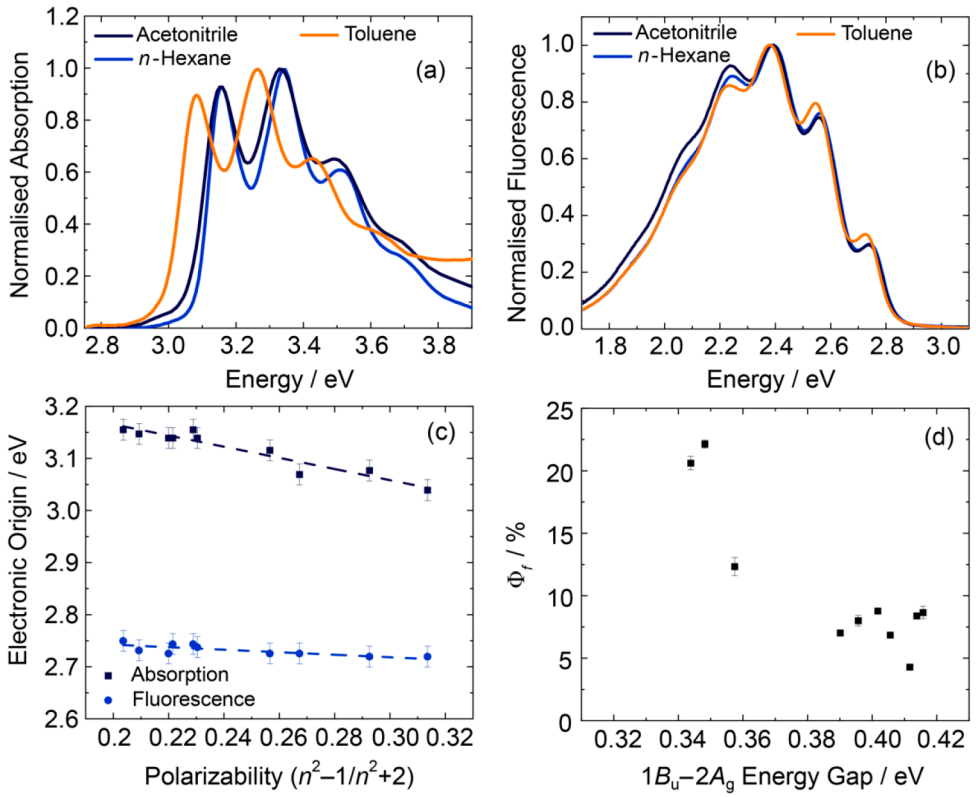

Figure 2. Normalized steady-state (a) absorption and (b) fluorescence spectra of DPO in three different solvents. (c) Absorption and fluorescence electronic origins derived from steady-state spectra as a function of solvent polarizability, $(n^2 - 1)/(n^2 + 2)$, where n is the refractive index of the solvent. (d) Experimentally determined fluorescence quantum yield (Φ_f) of DPO as a function of the estimated $1B_u$–$2A_g$ energy gap.

diphenylbutadiene, the prevailing consensus is that the $1B_u$ bright electronic state is the lowest energy singlet state.[26−28] The relative ordering of the first two excited states in the vertical Franck−Condon region is thought to invert at N ∼3−4—see Figure 1a. For "long" polyenes ($N \geq 5$), such as photosynthetic carotenoids, the $2A_g$ state is the lowest energy singlet excited state[1−3,13,23] and is populated by rapid internal conversion from the photoexcited $1B_u$ state.

The situation is less clear for polyenes with intermediate conjugation lengths (N ∼3−4), where it is expected that the $1B_u$ and $2A_g$ state energies will be energetically close,[24,25] e.g., for diphenylpolyenes such as diphenylhexatriene (DPH) and diphenyloctatetraene (DPO). DPH has received considerable attention due to its rich photophysics,[10,11,17−19,22,29−32] use as a fluorescent sensor,[33,34] and utilization in solar energy applications.[35−38] There are competing reports of the excited state dynamics of DPH.[10,22,29] It has been proposed that absorption and fluorescence do not occur from the same state in DPH.[10] While absorption occurs to the strongly allowed $1B_u$ state, fluorescence occurs on a nanosecond time scale (with appreciable quantum yields) from the formally optically dark $2A_g$ state. The latter state gains oscillator strength via Herzberg−Teller vibronic intensity borrowing from the strongly allowed $1B_u$ state.[39] In this proposed model, vibrations of b_u symmetry distort the molecular structure, relaxing the symmetry requirements and allowing the $2A_g$ state to fluoresce. The above proposed model for DPH is still debated, with one hypothesis that the $2A_g$ state is not involved in the excited state deactivation,[22] and the large observed Stokes shift and lack of mirror symmetry between absorption and fluorescence can be rationalized by a significant excited state geometric rearrangement.

Conversely, the photophysics of DPO, which has an additional double bond along the polyene backbone (chemical structure given in Figure 1b), has been far less intensively studied than DPH, with only a few studies to date examining the sub-nanosecond dynamics,[31,40−42] the fluorescence quantum yield,[43,44] and the nanosecond kinetics[18,41,44] in only weakly interacting solvents. Given the longer chain length, it is anticipated that the $1B_u$–$2A_g$ energy gap will be larger in DPO than DPH and strongly influence the excited state photophysics and associated fluorescence quantum yield. To comprehensively investigate the photophysical dynamics of DPO, steady-state and wavelength-resolved fluorescence lifetime spectroscopies were used to investigate how the dynamics varied in 10 solvents of different polarities and polarizabilities, e.g., ranging from weakly interacting solvents such as cyclohexane to polar hydrogen-bonding solvents such as methanol.

2. EXPERIMENTAL AND COMPUTATIONAL METHODS

2.1. Sample Preparation and Steady-State Spectroscopy. DPO (99%) was purchased from BOC Sciences and used without any further purification. DPO was dissolved in 10 different solvents purchased from Sigma-Aldrich (>99% purity). For fluorescence quantum yield and wavelength-resolved time-correlated single photon counting (WR-TCSPC) measurements, the solutions were diluted to have an absorbance of ∼0.1 and ∼0.3 at the peak wavelength of the pump laser in a static 1 cm path length cuvette, respectively.

https://doi.org/10.1021/acs.jpcb.3c03737
J. Phys. Chem. B 2023, 127, 8199−8207

Each sample was freshly prepared before ultrafast measurements. The fluorescence quantum yield of DPO in the various solvents was determined using an Edinburgh Instruments FS5 fluorimeter and SC-30 integrating sphere.

2.2. Wavelength-Resolved Time-Correlated Single Photon Counting Measurements. WR-TCSPC measurements were acquired using a modified version of the home-built TCSPC apparatus previously reported.[45] The output of a tunable high-power ultrafast oscillator (Chameleon Ultra II, 3.7 W, 80 MHz, Coherent) was frequency doubled to generate the required UV excitation pulses (392−408 nm). To avoid re-excitation of samples, the repetition rate was reduced to 6.67 MHz using a pulse picker (APE cavity dumper). The diffracted output was spatially filtered with a pinhole to remove residual zeroth order diffraction, and the resulting <15 pJ (per pulse) UV light was focused into a static liquid sample (1 cm path length cell). Fluorescence was collected at 90° relative to excitation using an infinity-corrected microscope objective (4×/0.2 NA Plan Apochromat, Nikon) and through a series of achromatic lenses collimated and focused onto an avalanche photodiode detector (ID100-50-ULN, IDQ).

Photon count arrival times were recorded with a time-to-digital converter (Time Tagger 20, Swabian Instruments) and accumulated in 10 ps bins. To facilitate wavelength-resolved TCSPC measurements, fluorescence was propagated through a birefringent interferometer (Gemini, Nireos)[46] after the collection objective and before the detector. Each data point was integrated for 1 s, and every spectral interferogram was averaged 10 times. All WR-TCSPC data were acquired by using customized LabVIEW software (National Instruments). Spectral filtering due to transmission through the collecting objective and Gemini interferometer was corrected for in postprocessing. The instrument response function (IRF) was 170 ps, as determined by recording laser scatter from solvent in a 1 cm path length cuvette. The wavelength dependence characterization of the IRF is given in the Supporting Information (see Figure S4). All data were collected at room temperature (20 °C) using the magic angle condition.

2.3. Density Functional Theory Calculations. Density functional theory (DFT) and time-dependent DFT (TD-DFT) calculations were performed using the Gaussian 16 computational suite.[47] The minimum energy geometries of the ground electronic state and optically bright excited state were calculated by using the ωB97-XD exchange-correlation density functional and the def2-SVP basis set. Solvation effects were included in vertical excitation energy calculations using a polarizable continuum model.

3. RESULTS AND DISCUSSION

3.1. Steady-State Spectroscopy. The steady-state absorption and fluorescence spectra of DPO in acetonitrile, *n*-hexane, and toluene are shown in Figure 2a,b. Focusing first on the solvent-dependent absorption spectra (Figure 2a), the absorption spectra shift to lower energy with increasing solvent polarizability, however, seemingly without any major change in line shape. Making the reasonable assumption that the lowest energy vibronic peak in these data corresponds to the $1B_u$ electronic origin (0−0 band), a linear trend was found as a function of the solvent polarizability (α, commonly modeled as $(n^2 - 1)/(n^2 + 2)$),[48] as shown in Figure 2c, with similar trends reported for many polyenes previously.[11,23,49,50]

The polarization-dependent excitation energies take the form of a linear slope[10]

$$\nu_i = \nu_i^0 - \alpha P_i \quad (1)$$

where ν_i and ν_i^0 are the solution phase and gas phase excitation energies associated with the *i*th electronic state. The gradient, P_i, is related to the associated electronic transition dipole moment of the electronic state, and thus, higher oscillator strength transitions are expected to exhibit greater polarizability-dependent solvatochromic shifts.

Fitting the data in Figure 2c to eq 1 results in gradients of 2000 ± 500 and 9000 ± 1000 cm^{-1} for the $2A_g$ and $1B_u$ states, respectively. Extrapolation of these fits to zero polarizability allows the gas phase energy gap between the two states to be estimated as 4600 ± 2200 cm^{-1}. These values are used to calculate the differential solvation and energy gap of the two electronic states in section 3.2.

To investigate whether the low-energy portion of the absorption spectra (2.8−3.5 eV) is dominated by vibronic transitions to a single electronic state, the experimental absorption spectra were modeled using a Franck−Condon progression for a single harmonic oscillator.[51,52] Full details, including the limitations of the model, are given in section 1 of the Supporting Information. Using this model, experimental spectra were reproduced with excellent agreement using a single Franck−Condon active vibrational wavenumber of 1520 ± 10 cm^{-1} most likely corresponding to a C=C stretching nuclear mode[12,53,54] and an associated Huang−Rhys factor (S) of 1.27. Across the different solvents, only the 0−0 band energy was altered in the modeled fit to capture the solvatochromic shift. The success of the displaced harmonic oscillator model to reproduce the experimental absorption spectra confirms that long-wavelength absorption is dominated by, or solely attributable to, a single electronic transition in all 10 solvents.

To support the experimental observations, density functional theory (DFT) and time-dependent (TD)-DFT calculations were conducted on the $1A_g$ and $1B_u$ electronic states initially in the gas phase. The $2A_g$ state was not investigated, as TD-DFT is unable to properly capture the expected doubly excited nature of this transition.[55,56] Geometry optimization of the ground state with DFT returned a planar geometry—the associated structure and bond lengths are shown in Figure S3a, displaying a strong alternation of the C=C (1.35 Å) and C—C (1.45 Å) bond lengths along the DPO backbone, in line with prior computational studies of polyenes.[25,57,58] TD-DFT vertical excitation calculations predict that the $1B_u$ state has a very large oscillator strength (f = 2.567). TD-DFT optimization of the $1B_u$ excited state returned a planar geometry, with near identical bond lengths (1.40 Å, Figure S2a) associated with the central linear carbon chain of DPO, and some minor alternation toward the terminal phenyl rings (1.39/1.40 Å), in accord with prior findings.[25,57,58] The solvatochromic shift in the $1B_u$ origin observed experimentally was modeled in TD-DFT calculations by the inclusion of a polarizable continuum solvent model in the vertical excitation energies. The results of these calculations are shown overlaid with experimental results in Figure S3 and yield a quantitatively similar trend.

The fluorescence spectra for DPO in *n*-hexane, toluene, and acetonitrile are shown in Figure 2b. Compared to the respective absorption data (Figure 2a), the fluorescence spectra do not mirror the absorption spectral line shape and also fail to exhibit the same strong polarizability-dependent solvatochromic shift (Figure 2c). The fluorescence spectra

https://doi.org/10.1021/acs.jpcb.3c03737
J. Phys. Chem. B 2023, 127, 8199−8207

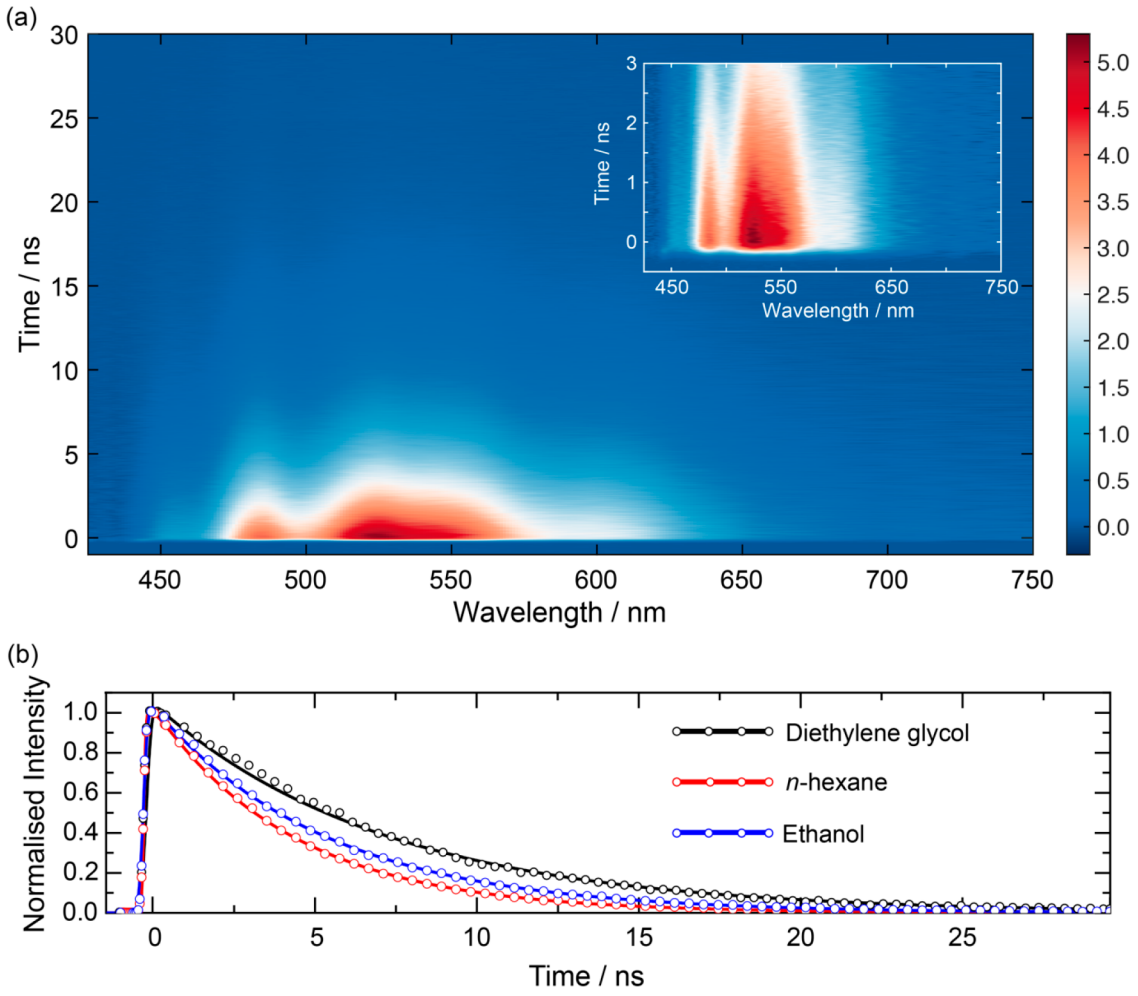

Figure 3. (a) WR-TCPSC false color contour map of DPO in *n*-hexane. The inset shows the first few nanoseconds of the fluorescence decay. (b) Example fluorescence decay kinetics (dots, sampled every 400 ps) for DPO in room temperature ethanol, *n*-hexane, and diethylene glycol and overlaid fits (solid lines).

were successfully modeled using the same approach outlined above for absorption, with a Franck−Condon progression in a single vibrational mode of wavenumber 1390 ± 10 cm^{-1}, with S varying between 2.27 and 2.45 across the 10 solvents (<10%). Such a variation in the Huang−Rhys factor is likely an indicator of small changes in displacement of the fluorescent state potential energy minima.[51,59,60] The ability of the model to reproduce the fluorescence profiles indicates that the fluorescence originates primarily from a single excited state. The lack of mirror symmetry between absorption and fluorescence spectra and different solvatochromic behavior supports the hypothesis that fluorescence occurs from a different electronic state than initially excited. Therefore, in agreement with other studies,[10,18,40] DPO fluorescence dominantly originates from the $2A_g$ state. Prior studies have reported very weak additional bands in fluorescence spectra (at shorter wavelengths than the main band) associated with the $1B_u$ state;[40,61] however, these were not observed in the present study.

As determined above, the vast majority of DPO fluorescence originates from the formally dipole forbidden $2A_g$ state and, therefore like other polyenes, must gain oscillator strength via Herzberg−Teller intensity borrowing from the proximal optically bright $1B_u$ state. For this mechanism to be effective, it requires strong coupling between the bright and dark electronically excited states, which is directly dependent on their relative minimum energies.[10] Due to the differential solvent stabilization of the two lowest energy excited states of DPO, the $1B_u$−$2A_g$ energy gap can be controlled by small changes in the solvent polarizability.

The DPO fluorescence quantum yield as a function of the estimated $1B_u$−$2A_g$ state energy gap is displayed in Figure 2d, and a negative trend is observed. Overall, the fluorescence quantum yield varies between 4.3 and 21.2%, with a mean of 5.7% and standard deviation of 10.6%. However, as the fluorescence yield is not close to unity, there must be competitive non-radiative excited state deactivation pathways, which may also vary as a function of solvent and affect the fluorescence quantum yield. To further investigate the excited state dynamics of DPO, wavelength-resolved time-correlated single photon counting (WR-TCSPC) measurements were undertaken.

3.2. WR-TCSPC. The wavelength-resolved time-correlated fluorescence spectrum of DPO in *n*-hexane is displayed in Figure 3a. There were no apparent shifts in the fluorescence line shape observed outside of the IRF in any solvent, and the fluorescence intensity decayed monotonically. Spectral slices for several different time delays are shown in Figure S5 for DPO dissolved in *n*-hexane and ethanol. Figure 3b shows representative kinetics obtained by averaging over the entire

https://doi.org/10.1021/acs.jpcb.3c03737
J. Phys. Chem. B 2023, 127, 8199−8207

Table 1. Experimentally Determined DPO Fluorescence Quantum Yield (Φ_f), Fluorescence Lifetime (τ_f), Derived Fluorescence Rate Constant (k_f), Absorption, and Fluorescence Origins in 10 Different Solvents

Solvent	$(n^2-1)/(n^2+2)$	Φ_f/%	τ_f/ns	$k_f/\times 10^7$ s^{-1}	Absorption origin/eV	Fluorescence origin/eV
methanol	0.204	6.9 ± 0.2	5.07 ± 0.17	1.35 ± 0.05	3.16 ± 0.02	2.75 ± 0.02
acetonitrile	0.209	8.7 ± 0.5	5.13 ± 0.17	1.69 ± 0.06	3.15 ± 0.02	2.73 ± 0.02
acetone	0.220	8.4 ± 0.2	5.11 ± 0.17	1.64 ± 0.05	3.14 ± 0.02	2.73 ± 0.02
ethanol	0.221	8.0 ± 0.5	5.38 ± 0.17	1.49 ± 0.05	3.14 ± 0.02	2.74 ± 0.02
n-hexane	0.229	4.3 ± 0.1	4.29 ± 0.17	0.99 ± 0.04	3.16 ± 0.02	2.74 ± 0.02
2-propanol	0.230	8.8 ± 0.2	5.19 ± 0.17	1.69 ± 0.06	3.14 ± 0.02	2.74 ± 0.02
cyclohexane	0.257	7.0 ± 0.1	5.36 ± 0.17	1.31 ± 0.04	3.12 ± 0.02	2.73 ± 0.02
diethylene glycol	0.267	20.6 ± 0.5	7.21 ± 0.17	2.86 ± 0.07	3.07 ± 0.02	2.73 ± 0.02
toluene	0.293	12.3 ± 0.7	4.87 ± 0.17	2.54 ± 0.09	3.08 ± 0.02	2.72 ± 0.02
benzyl alcohol	0.314	21.2 ± 1.4	6.53 ± 0.17	3.25 ± 0.08	3.04 ± 0.02	2.72 ± 0.02

emission band for three solvents. Overlaid are fits to the data modeled as a monoexponential decay convolved with a Gaussian IRF function. The time constants returned from fitting to the experimental time-resolved fluorescence data are listed in Table 1.

The lack of a wavelength dependence on the fluorescence decay kinetics measured in all solvents is in agreement with steady-state measurements and indicates that all the observed fluorescence originates from the $2A_g$ state. This necessitates that the internal conversion transfer from the $1B_u$ state must be rapid and complete in a time scale shorter than the instrumental response (170 ps). Previous studies disagree on the time scale for $1B_u \rightarrow 2A_g$ interconversion in DPO reporting time constants of <1 ps and hundreds of ps.[31,40−42] Our results are in accord with the prompter interconversion time scale.

The time-resolved fluorescence data are dominated by a monoexponential decay, with solvent-dependent nanosecond lifetimes, which are presented in Table 1. There is a significant variation in fluorescence lifetime, which falls within the range 4.29−7.21 ns, and has a mean value of 5.41 ns and 0.84 ns standard deviation. The monoexponential fluorescence decay observed for DPO contrasts with the biexponential nanosecond fluorescence dynamics previously observed in similar chain length polyenes such as diphenylbutadiene (DPB)[62] and DPH,[63] indicating far simpler dynamics in this longer chain diphenylpolyene.

Rather than analyzing the fluorescence lifetimes, these data were converted into fluorescence rates (k_f) using the fluorescence quantum yield and fluorescence lifetime as defined in eqs 2 and 3

$$\Phi_f = \frac{k_f}{k_f + \sum k_{NR}} \tag{2}$$

$$\tau_f = \frac{1}{k_f + \sum k_{NR}} \tag{3}$$

which via substitution yields

$$k_f = \frac{\Phi_f}{\tau_f} \tag{4}$$

where Φ_f is the fluorescence quantum yield, Σk_{NR} is the sum of non-radiative rate constants, and τ_f is the fluorescence lifetime derived from fits to WR-TCSPC data.

Andrews and Hudson,[10] following the work of Hug and Becker,[64] derived an expression for the fluorescence rate of a forbidden electronic state mediated by vibronic intensity borrowing based on perturbation theory—an adapted form is given in eq 5

$$K_f = \frac{(n^2+2)^2}{9n^2}k_f = \frac{\Gamma^2}{(\Delta E^0 - \alpha \Delta P)^2} \tag{5}$$

where K_f is the radiative rate of the formally dipole forbidden state corrected for the local field; e.g., in the gas phase, α, n, and k_f are defined earlier. The remaining three parameters in eq 5 are variables: ΔE^0 corresponds to the energy gap between the $1B_u$ and $2A_g$ states in the gas phase, ΔP is the differential solvation between the two electronic states, and both quantities can be estimated as discussed in section 3.1. Γ^2 is a collection of molecular specific terms:

$$\Gamma^2 = \frac{2\omega^3}{hc^3} m^2 {h_{BA}}^2 \tag{6}$$

In eq 6, ω is the central fluorescence wavelength, h is Planck's constant, c is the speed of light, m is the transition dipole moment of the $1B_u$ state, and h_{BA} is the vibronic coupling term between the optically bright and dark states.

Andrews and Hudson's model[10] presumed the solvent has no direct effect on the solute and would thus be unable to promote non-totally symmetric distortions. This approximation is most appropriate for non-polar solvents with low permanent dipole moments. In polar solvents, the effect of the solvent permanent dipole in the immediate region surrounding the solute will have a more significant effect. This instantaneous interaction will promote greater non-totally symmetric distortions in the solute which are not a result of vibronic mixing. This effect is solely due to direct interactions with the solvent and is independent of the solvent polarizability. As a result, it is expected that the radiative rates determined for polar solvents (with higher dielectric constants) will be greater than those in non-polar solvents due to the non-totally symmetric distortions in the DPO nuclear framework generated by the solvent.

All measurements were acquired in solution and thus were corrected for the local solvent field $(n^2+2)^2/9n^2$, as derived previously.[65] Figure 4 shows the corrected fluorescence rates (K_f) as a function of solvent polarizability, with close to quadratic behavior evident. Two trends were evident for solvents with high (ε < 15) and low (ε > 15) dielectric constants.

Evaluation of the model outlined in eq 5 yielded a good agreement with the experimental data; see overlaid models with experimental data in Figure 4. The modeling returns three quantities, ΔE^0, Γ^2, and h_{BA}. To obtain a good fit to data, ΔE^0

https://doi.org/10.1021/acs.jpcb.3c03737
J. Phys. Chem. B 2023, 127, 8199−8207

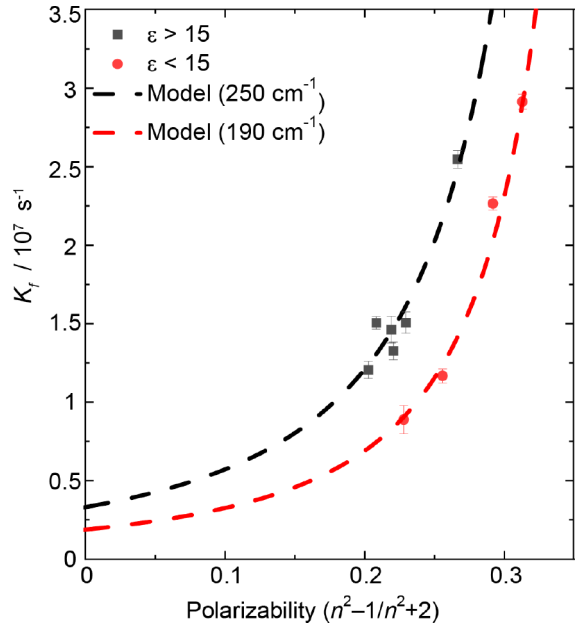

Figure 4. Measured radiative rate corrected for local solvent effects as a function of the solvent polarizability. Overlaid dashed lines correspond to the results of the intensity borrowing model discussed in the main text for the two solvent dielectric regimes.

was allowed to vary within the range determined in section 3.1, with 3350 cm^{-1} returned from modeling. This value is in reasonable agreement with gas phase measurements of DPO which estimated the $1B_u$–$2A_g$ energetic gap to be ∼4000 cm^{-1}.[66] The differential solvation parameter returned from the evaluation of eq 5 gave a value of 8000 cm^{-1}, which is within the bounds determined in section 3.1 (7000 ± 1000 cm^{-1}). Finally, from the returned value of Γ^2 it is possible to extract a vibronic coupling constant using eq 6 and the $1B_u \leftarrow 1A_g$ transition dipole moment calculated using TD-DFT (13.75 D). Using this method, h_{BA} values were estimated to be 250 and 190 cm^{-1} for high and low polarity solvents, respectively. This value is reasonable for intensity borrowing (∼hundreds of cm^{-1})[10] and is consistent with those previously calculated for other polyenes—DPH and retinol are estimated to have vibronic coupling constants of 555 and 149 cm^{-1}, respectively.[10] Further, as expected, the high polarity data requires a larger coupling constant likely due to the increased non-totally symmetric vibrations induced by interactions with the solvent, which are not fully accounted for in the simplistic static term used to correct for the local field. Therefore, the 190 cm^{-1} coupling constant obtained from solvents of low dielectric constants is the most reliable value determined. The success of Andrews and Hudson's model is strong evidence to support the hypothesis that the vast majority of DPO fluorescence originates from the $2A_g$ state and that the electronic state gains oscillator strength via vibronic intensity stealing from the $1B_u$ state.

There are important parallels and differences between the observed photophysics of DPO revealed in the present study and the prior investigations of related polyene DPH. The fluorescence quantum yield for DPO varies between 4.3 and 21.2% and increases as a function of the solvent polarizability (Table 1). The room temperature fluorescence quantum yield of DPH has only been recorded in a smaller range of solvents such as saturated alkanes where the channel is far more important (62–65%) than in DPO. However, in less polarizable and polar solvents such as ethanol and acetonitrile the fluorescence quantum yield of DPH (15–25%)[11] is similar to the maximum fluorescence yield in DPO.

Regardless of the solvent, there is a large percentage of excited DPO (and DPH) molecules that do not relax via fluorescence, leaving much of the excited state dynamics unaccounted for. An intersystem crossing pathway can be excluded as prior photosensitization experiments reported triplet quantum yields for DPH and DPO of <1% in conventional polar and non-polar solvents.[67] Therefore, photoexcited molecules that do not fluoresce must either internally convert directly to the electronic ground state from the $2A_g$[2] or $1B_u$ states[68] or alternatively photoisomerize as reported for DPO, DPH, and also DPB.[43] The quantum yield for *trans* → *cis* photoisomerization of DPH is 36% in acetonitrile, a solvent with a correspondingly modest (25%) fluorescence quantum yield.[29] The photoisomerization yields have, to the best of our knowledge, not been reported for DPO, but given the structural similarity with DPH we speculate that this must also be a key non-radiative excited state decay channel for DPO in all solvents given the fairly low (<22%) fluorescence quantum yield.

One important factor that will determine whether fluorescence is the most competitive decay pathway for the $2A_g$ state of diphenylpolyenes compared to other non-radiative pathways is the radiative rate, which for the formally dipole forbidden electronic transition that gains oscillator strength via intensity borrowing is inversely proportional to $[\Delta E^0(1B_u - 2A_g)]^2$—see eq 5. We have determined ΔE^0 for DPO (via extrapolation from steady-state data) to be 4600 cm^{-1}, which is ∼1/3 greater than the energy gap for DPH (3410 cm^{-1}).[32] The differences in ΔE^0 help to reconcile the 2–3× greater radiative rates reported for DPH[11] compared to those determined here for DPO.

4. CONCLUSIONS

The photophysics of DPO have been comprehensively studied, in a far wider range of solvents than previously investigated, ranging from weakly interacting non-polar solvents to hydrogen-bonding alcohols. These studies utilized steady-state absorption and fluorescence spectroscopies alongside wavelength-resolved time-correlated single photon counting measurements to establish a more detailed model for the excited state dynamics of DPO than hitherto reported. These data reveal that photoexcitation to the $1B_u$ state of DPO leads to fast (<170 ps) internal conversion to the lower-lying optically dark $2A_g$ state in agreement with some prior studies.[31,41,42] The $2A_g$ state is responsible for the vast majority of fluorescence and gains oscillator strength via intensity borrowing from the optically bright $1B_u$ state. The Herzberg–Teller vibronic coupling constant between the $1B_u$ and $2A_g$ states was estimated to be 190 cm^{-1}. The wavelength-resolved time-dependent fluorescence data show no spectral evolution within our time resolution but reveal that the $2A_g$ state fluoresces back to the ground state monotonically, in contrast to prior observations of DPH and DPB which exhibit biphasic fluorescence decay from the lowest excited singlet state.[26,63] These studies demonstrate that the electronic state ordering must be conserved in all of the solvents studied, and the $2A_g$ minimum is always lower in energy than that of the corresponding $1B_u$ state. The maximum fluorescence quantum yield was found to be 21% in benzyl alcohol solution—the

https://doi.org/10.1021/acs.jpcb.3c03737
J. Phys. Chem. B 2023, 127, 8199–8207

most polarizable solvent studied. As a result, this means the majority of photoexcited DPO molecules decay from the excited state via alternative non-radiative decay pathways including *trans* → *cis* photoisomerization and potentially direct internal conversion to the ground electronic state. As evident from the data presented, the fluorescence rate and quantum yield of DPO are very sensitive, in a predictable manner, to the refractive index of the environment, due to the photophysical model proposed. The net result is the environmental sensitivity of DPO, utilized for *in vivo* fluorescent bioimaging, can be rationalized with fundamental molecular photophysics.

■ ASSOCIATED CONTENT

Supporting Information

The Supporting Information is available free of charge at https://pubs.acs.org/doi/10.1021/acs.jpcb.3c03737.

Franck−Condon factor modeling; TCSPC instrument response function; slices of wavelength-resolved TCSPC data; minimum energy DFT and TD-DFT structures; and calculated and experimental $1B_u$ excitation energies (PDF)

■ AUTHOR INFORMATION

Corresponding Author

Thomas A. A. Oliver − *School of Chemistry, Cantock's Close, University of Bristol, Bristol BS8 1TS, U.K.;* orcid.org/0000-0003-3979-7857; Email: tom.oliver@bristol.ac.uk

Authors

Daniel W. Polak − *School of Chemistry, Cantock's Close, University of Bristol, Bristol BS8 1TS, U.K.;* Present Address: Department of Chemistry, University of Leicester, Leicester LE1 7RH, U.K; orcid.org/0000-0002-6479-2225

Alexandros D. P. Hannon − *School of Chemistry, Cantock's Close, University of Bristol, Bristol BS8 1TS, U.K.*

Guilherme A. Marczak Giorio − *School of Chemistry, Cantock's Close, University of Bristol, Bristol BS8 1TS, U.K.*

Olivia A. Hawkins − *School of Chemistry, Cantock's Close, University of Bristol, Bristol BS8 1TS, U.K.*

Complete contact information is available at: https://pubs.acs.org/10.1021/acs.jpcb.3c03737

Notes

The authors declare no competing financial interest.

Data are available from the University of Bristol data repository at https://doi.org/10.5523/bris.1qq9ffnrwc5gl2jc27ip9jog75.

■ ACKNOWLEDGMENTS

The authors thank Basile Curchod and Dasha Shchepanovska for useful discussions. Financial support is acknowledged from EPSRC for the award of Programme Grant EP/V026690/1. T.A.A.O. acknowledges the Royal Society for a University Research Fellowship (URF\R\201007) and Research Fellows Enhancement Award (RF\ERE\210045).

■ REFERENCES

(1) Frank, H. A.; Cogdell, R. J. Carotenoids in Photosynthesis. *Photochem. Photobiol.* **1996**, *63* (3), 257−264.

(2) Polívka, T.; Sundström, V. Ultrafast Dynamics of Carotenoid Excited States−From Solution to Natural and Artificial Systems. *Chem. Rev.* **2004**, *104* (4), 2021−2072.

(3) Polívka, T.; Sundström, V. Dark Excited States of Carotenoids: Consensus and Controversy. *Chem. Phys. Lett.* **2009**, *477* (1−3), 1−11.

(4) Blankenship, R. E. *Molecular Mechanisms of Photosynthesis*; Wiley-Blackwell: 2010.

(5) *Non-Photochemical Quenching and Energy Dissipation in Plants, Algae and Cyanobacteria*; Demmig-Adams, B., Garab, G., Adams, W., III, Govindjee, Eds.; Springer: 2014.

(6) Bode, S.; Quentmeier, C. C.; Liao, P.-N.; Hafi, N.; Barros, T.; Wilk, L.; Bittner, F.; Walla, P. J. On the Regulation of Photosynthesis by Excitonic Interactions between Carotenoids and Chlorophylls. *Proc. Natl. Acad. Sci. U.S.A.* **2009**, *106* (30), 12311−12316.

(7) Hashimoto, H.; Uragami, C.; Yukihira, N.; Gardiner, A. T.; Cogdell, R. J. Understanding/Unravelling Carotenoid Excited Singlet States. *J. R. Soc. Interface* **2018**, *15* (141), 20180026.

(8) Frank, H. A.; Cua, A.; Chynwat, V.; Young, A.; Gosztola, D.; Wasielewski, M. R. Photophysics of the Carotenoids Associated with the Xanthophyll Cycle in Photosynthesis. *Photosynth. Res.* **1994**, *41* (3), 389−395.

(9) Zigmantas, D.; Hiller, R. G.; Sharples, F. P.; Frank, H. A.; Sundström, V.; Polívka, T. Effect of a Conjugated Carbonyl Group on the Photophysical Properties of Carotenoids. *Phys. Chem. Chem. Phys.* **2004**, *6* (11), 3009−3016.

(10) Andrews, J. R.; Hudson, B. S. Environmental Effects on Radiative Rate Constants with Applications to Linear Polyenes. *J. Chem. Phys.* **1978**, *68* (10), 4587−4594.

(11) Cehelnik, E. D.; Cundall, R. B.; Lockwood, J. R.; Palmer, T. F. Solvent and Temperature Effects on the Fluorescence of All-Trans-1,6-Diphenyl-1,3,5-Hexatriene. *J. Phys. Chem.* **1975**, *79* (14), 1369−1376.

(12) Hudson, B. S.; Kohler, B. E. Polyene Spectroscopy: The Lowest Energy Excited Singlet State of Diphenyloctatetraene and Other Linear Polyenes. *J. Chem. Phys.* **1973**, *59* (9), 4984−5002.

(13) Hudson, B. S.; Kohler, B. E. A Low-Lying Weak Transition in the Polyene α,ω-Diphenyloctatetraene. *Chem. Phys. Lett.* **1972**, *14* (3), 299−304.

(14) Frank, H. A.; Christensen, R. L. *Carotenoids*, Vol. *4*; Britton, G., Liaaen-Jensen, S., Pfander, H., Eds.; Birkhäuser: 2008.

(15) Schulten, K.; Karplus, M. On the Origin of a Low-Lying Forbidden Transition in Polyenes and Related Molecules. *Chem. Phys. Lett.* **1972**, *14* (3), 305−309.

(16) Orlandi, G.; Zerbetto, F.; Zgierski, M. Z. Theoretical Analysis of Spectra of Short Polyenes. *Chem. Rev.* **1991**, *91* (5), 867−891.

(17) Parasassi, T.; Stasio, G. D.; Rusch, R. M.; Gratton, E. A Photophysical Model for Diphenylhexatriene Fluorescence Decay in Solvents and in Phospholipid Vesicles. *Biophys. J.* **1991**, *59* (2), 466−475.

(18) Brey, L. A.; Schuster, G. B.; Drickamer, H. G. High Pressure Fluorescence Studies of Radiative and Nonradiative Processes in Diphenyl Hexatriene, Diphenyl Octatetraene, and Retinyl Acetate. *J. Chem. Phys.* **1979**, *71* (7), 2765−2772.

(19) Küpper, B.; Kleinschmidt, M.; Schaper, K.; Marian, C. M. On the Photophysics of 1,6-Diphenyl-1,3,5-Hexatriene Isomers and Rotamers. *ChemPhysChem* **2011**, *12* (10), 1872−1879.

(20) Turek, A. M.; Krishnamoorthy, G.; Sears, D. F.; Garcia, I.; Dmitrenko, O.; Saltiel, J. Resolution of Three Fluorescence Components in the Spectra of All-Trans-1,6-Diphenyl-1,3,5-Hexatriene under Isopolarizability Conditions. *J. Phys. Chem. A* **2005**, *109* (2), 293−303.

(21) Alford, P. C.; Palmer, T. F. Fluorescence of Derivatives of All-Trans-1,6-Diphenyl-1,3,5-Hexatriene. *Chem. Phys. Lett.* **1986**, *127* (1), 19−25.

(22) Catalán, J. On the Temperature-dependent Isomerization of All-Trans-1,6-Diphenyl-1,3,5-Hexatriene in Solution: A Reappraisal. *J. Phys. Org. Chem.* **2022**, *35* (6), e4336.

(23) Christensen, R. L.; Galinato, M. G. I.; Chu, E. F.; Howard, J. N.; Broene, R. D.; Frank, H. A. Energies of Low-Lying Excited States of Linear Polyenes. *J. Phys. Chem. A* **2008**, *112* (49), 12629−12636.

(24) Tavan, P.; Schulten, K. Electronic Excitations in Finite and Infinite Polyenes. *Phys. Rev. B* **1987**, *36* (8), 4337−4358.
(25) Schmidt, M.; Tavan, P. Electronic Excitations in Long Polyenes Revisited. *J. Chem. Phys.* **2012**, *136* (12), 124309.
(26) Wallace-Williams, S. E.; Schwartz, B. J.; Moeller, S.; Goldbeck, R. A.; Yee, W. A.; El-Bayoumi, M. A.; Kliger, D. S. Excited State Spectra and Dynamics of Phenyl-Substituted Butadienes. *J. Phys. Chem.* **1994**, *98* (1), 60−67.
(27) Dahl, K.; Biswas, R.; Maroncelli, M. The Photophysics and Dynamics of Diphenylbutadiene in Alkane and Perfluoroalkane Solvents. *J. Phys. Chem. B* **2003**, *107* (31), 7838−7853.
(28) Krohn, O. A.; Quick, M.; Sudarkova, S. M.; Ioffe, I. N.; Richter, C.; Kovalenko, S. A. Photoisomerization Dynamics of *Trans*−*Trans*, *Cis*−*Trans*, and *Cis*−*Cis* Diphenylbutadiene from Broadband Transient Absorption Spectroscopy and Calculations. *J. Chem. Phys.* **2020**, *152* (22), 224305.
(29) Saltiel, J.; Krishnamoorthy, G.; Huang, Z.; Ko, D.-H.; Wang, S. Photoisomerization of All-Trans-1,6-Diphenyl-1,3,5-Hexatriene. Temperature and Deuterium Isotope Effects. *J. Phys. Chem. A* **2003**, *107* (18), 3178−3186.
(30) Itoh, T.; Kohler, B. E. Dual Fluorescence of Diphenylpolyenes. *J. Phys. Chem.* **1987**, *91* (7), 1760−1764.
(31) Yee, W. A.; O'Neil, R. H.; Lewis, J. W.; Zhang, J. Z.; Kliger, D. S. Femtosecond Transient Absorption Studies of Diphenylpolyenes. Direct Detection of $S_2 \rightarrow S_1$ Radiationless Conversion in Diphenylhexatriene and Diphenyloctatetraene. *Chem. Phys. Lett.* **1997**, *276* (5−6), 430−434.
(32) Kohler, B. E.; Spiglanin, T. A. Structure and Dynamics of Excited Singlet States of Isolated Diphenylhexatriene. *J. Chem. Phys.* **1984**, *80* (11), 5465−5471.
(33) Kellner, R. R.; Baier, C. J.; Willig, K. I.; Hell, S. W.; Barrantes, F. J. Nanoscale Organization of Nicotinic Acetylcholine Receptors Revealed by Stimulated Emission Depletion Microscopy. *Neuroscience* **2007**, *144* (1), 135−143.
(34) Kaiser, R. D.; London, E. Location of Diphenylhexatriene (DPH) and Its Derivatives within Membranes: Comparison of Different Fluorescence Quenching Analyses of Membrane Depth. *Biochemistry* **1998**, *37* (22), 8180−8190.
(35) Kim, H.; Zimmerman, P. M. Coupled Double Triplet State in Singlet Fission. *Phys. Chem. Chem. Phys.* **2018**, *20* (48), 30083−30094.
(36) Karmakar, N.; Das, M. Low-Lying Excited States of Diphenylpolyenes and Its Derivatives in Singlet Fission: A Density Matrix Renormalization Group Study. *Comput. Theor. Chem.* **2022**, *1217*, 113918.
(37) Millington, O.; Montanaro, S.; Leventis, A.; Sharma, A.; Dowland, S. A.; Sawhney, N.; Fallon, K. J.; Zeng, W.; Congrave, D. G.; Musser.; et al. Soluble Diphenylhexatriene Dimers for Intramolecular Singlet Fission with High Triplet Energy. *J. Am. Chem. Soc.* **2023**, *145* (4), 2499−2510.
(38) Huang, Y.; Buyanova, I. A.; Phansa, C.; Sandoval-Salinas, M. E.; Casanova, D.; Myers, W. K.; Greenham, N. C.; Rao, A.; Chen, W. M.; Puttisong, Y. Competition between Triplet Pair Formation and Excimer-like Recombination Controls Singlet Fission Yield. *Cell Rep. Phys. Sci.* **2021**, *2* (2), 100339.
(39) Herzberg, G. *Electronic Spectra and Electronic Structure of Polyatomic Molecules*; Van Nostrand: Princeton, NJ, 1967.
(40) Felder, T. C.; Chio, K.-J.; Topp, M. R. Picosecond Observation of Fluorescence from Bu States of Diphenylpolyenes. *Chem. Phys.* **1982**, *64* (2), 175−182.
(41) Bachilo, S. M.; Gillbro, T. Diphenyloctatetraene S_2 Emission. *Chem. Phys. Lett.* **1994**, *218* (5−6), 557−562.
(42) Kukura, P.; McCamant, D. W.; Davis, P. H.; Mathies, R. A. Vibrational Structure of the S_2 (^{1}Bu) Excited State of Diphenyloctatetraene Observed by Femtosecond Stimulated Raman Spectroscopy. *Chem. Phys. Lett.* **2003**, *382* (1−2), 81−86.
(43) Görner, H. Singlet Mechanism for Trans → Cis Photoisomerization of α, ω-Diphenylpolyenes in Solution: Laser Flash Study of the Triplet States of Diphenylbutadiene. *Diphenylhexatriene and Diphenyloctatetraene. J. Photochem.* **1982**, *19* (4), 343−356.
(44) Birks, J. B.; Dyson, D. J. The Relations between the Fluorescence and Absorption Properties of Organic Molecules. *Proc. R. Soc. London A* **1963**, *275* (1360), 135−148.
(45) Amoruso, G.; Liu, J.; Polak, D. W.; Tiwari, K.; Jones, M. R.; Oliver, T. A. A. High-Efficiency Excitation Energy Transfer in Biohybrid Quantum Dot−Bacterial Reaction Center Nanoconjugates. *J. Phys. Chem. Lett.* **2021**, *12* (23), 5448−5455.
(46) Perri, A.; Gaida, J. H.; Farina, A.; Preda, F.; Viola, D.; Ballottari, M.; Hauer, J.; Silvestri, S. D.; D'Andrea, C.; Cerullo, G.; Polli, D. Time- and Frequency-Resolved Fluorescence with a Single TCSPC Detector via a Fourier-Transform Approach. *Opt. Express* **2018**, *26* (3), 2270−2279.
(47) Frisch, M. J.; Trucks, G. W.; Schlegel, H. B.; Scuseria, G. E.; Robb, M. A.; Cheeseman, J. R.; Scalmani, G.; Barone, V.; Petersson, G. A.; Nakatsuji, H.; et al. *Gaussian 16*, revision C.01; Gaussian, Inc.: Wallingford, CT, 2016.
(48) McRae, E. G. Theory of Solvent Effects on Molecular Electronic Spectra. Frequency Shifts. *J. Phys. Chem.* **1957**, *61* (5), 562−572.
(49) Nagae, H.; Kuki, M.; Cogdell, R. J.; Koyama, Y. Shifts of the $^1A^-_g \rightarrow {}^1B^+_u$ Electronic Absorption of Carotenoids in Nonpolar and Polar Solvents. *J. Chem. Phys.* **1994**, *101* (8), 6750−6765.
(50) Macpherson, A. N.; Gillbro, T. Solvent Dependence of the Ultrafast S_2−S_1 Internal Conversion Rate of β-Carotene. *J. Phys. Chem. A* **1998**, *102* (26), 5049−5058.
(51) Saidani, M. A.; Benfredj, A.; Hamed, Z. B.; Romdhane, S.; Ulbricht, C.; Egbe, D. A. M.; Bouchriha, H. Franck-Condon Analysis of the Photoluminescence Spectra of a Triple-Bond Containing Polymer as a Solution and as a Thin Film. *Synth. Met.* **2013**, *184*, 83−85.
(52) Köhler, A.; Bässler, H. *Electronic Processes in Organic Semiconductors*; Wiley-VCH Verlag GmbH & Co. KGaA: Weinheim, Germany, 2015.
(53) Ikeyama, T.; Azumi, T. The Fluorescence and the Absorption Spectra of 1,8-diphenyl-1,3,5,7-octatetraene. The Origin of the Transition Moments and the Interpretation of Anomalous Intensity Distribution. *J. Chem. Phys.* **1982**, *76* (12), 5672−5677.
(54) Henneker, W. H.; Siebrand, W.; Zgierski, M. Z. Quantitative Interpretation of the Absorption and Emission Spectra of 1,8-Diphenyl-1,3,5,7-Octatetraene. *J. Chem. Phys.* **1983**, *79* (5), 2495−2496.
(55) Kleinschmidt, M.; Marian, C. M.; Waletzke, M.; Grimme, S. Parallel Multireference Configuration Interaction Calculations on Mini-β-Carotenes and β-Carotene. *J. Chem. Phys.* **2009**, *130* (4), No. 044708.
(56) Elliott, P.; Goldson, S.; Canahui, C.; Maitra, N. T. Perspectives on Double-Excitations in TDDFT. *Chem. Phys.* **2011**, *391* (1), 110−119.
(57) Fuß, W.; Haas, Y.; Zilberg, S. Twin States and Conical Intersections in Linear Polyenes. *Chem. Phys.* **2000**, *259* (2−3), 273−295.
(58) Kawashima, Y.; Nakayama, K.; Nakano, H.; Hirao, K. Theoretical Study of the $\pi \rightarrow \pi^*$ Excited States of Linear Polyenes: The Energy Gap between $1^1B_u^+$ and $2^1A_g^-$ States and Their Character. *Int. J. Quantum Chem.* **1997**, *66*, 157−175.
(59) Spano, F. C.; Silva, C. H- and J-Aggregate Behavior in Polymeric Semiconductors. *Annu. Rev. Phys. Chem.* **2014**, *65* (1), 477−500.
(60) Spano, F. C. The Spectral Signatures of Frenkel Polarons in H- and J-Aggregates. *Acc. Chem. Res.* **2010**, *43* (3), 429−439.
(61) Itoh, T. Evaluation of the Coupling Constants between the 2^1A_g (S_1) and 1^1B_u (S_2) States for Diphenylhexatriene and Diphenyloctatetraene. *Chem. Phys. Lett.* **1989**, *159* (2−3), 263−266.
(62) Møller, S.; Yee, W. A.; Goldbeck, R. A.; Wallace-Williams, S. E.; Lewis, J. W.; Kliger, D. S. Biexponential Fluorescence Decay of Diphenylbutadiene Rotational Conformers after Extreme Red Edge Excitation. *Chem. Phys. Lett.* **1995**, *243* (5−6), 579−585.

https://doi.org/10.1021/acs.jpcb.3c03737
J. Phys. Chem. B 2023, 127, 8199−8207

(63) Hawkins, O. A. Investigating the Excited State Dynamics of 1,6-Diphenyl-1,3,5-Hexatriene Using Time Correlated Single Photon Counting; University of Bristol, 2021.
(64) Hug, G.; Becker, R. S. Solvent and Temperature Effects on Natural Radiative Lifetimes of Some Substituted Polyenes. *J. Chem. Phys.* **1976**, *65* (1), 55−63.
(65) Chako, N. Q. Absorption of Light in Organic Compounds. *J. Chem. Phys.* **1934**, *2* (10), 644−653.
(66) Itoh, T. Photophysics of α,ω-Diphenyloctatetraene in the Vapor Phase. *J. Phys. Chem. A* **2007**, *111* (18), 3502−3506.
(67) Chattopadhyay, S. K.; Das, P. K.; Hug, G. L. Photoprocesses in Diphenylpolyenes. Oxygen and Heavy-Atom Enhancement of Triplet Yields. *J. Am. Chem. Soc.* **1982**, *104* (17), 4507−4514.
(68) Oliver, T. A. A.; Fleming, G. R. Following Coupled Electronic-Nuclear Motion through Conical Intersections in the Ultrafast Relaxation of β-Apo-8′-Carotenal. *J. Phys. Chem. B* **2015**, *119* (34), 11428−11441.

https://doi.org/10.1021/acs.jpcb.3c03737
J. Phys. Chem. B 2023, 127, 8199−8207